Desalination and Water Treatment
www.deswater.com

doi: 10.1080/19443994.2016.1145605

57 (2016) 25097–25113
November

Taylor & Francis
Taylor & Francis Group

Biosorption of hexavalent chromium from aqueous solution using raw and acid-treated biosorbent prepared from *Lantana camara* fruit

K. Nithya[a,*], Asha Sathish[b], P. Senthil Kumar[c], T. Ramachandran[b]

[a]*Department of Chemical Engineering & Material Science, Amrita School of Engineering, Amrita Vishwa Vidyapeetham (University), Coimbatore 641 112, India, Tel. +91 9443477623; email: nithiamrita@gmail.com*
[b]*Department of Sciences (Chemistry), Amrita School of Engineering, Amrita Vishwa Vidyapeetham (University), Coimbatore 641 112, India, Tel. +91 9943977361; email: s_asha@cb.amrita.edu (A. Sathish), Tel. +91 9442006690; email: t_ramachandran@cb.amrita.edu (T. Ramachandran)*
[c]*Department of Chemical Engineering, SSN College of Engineering, Chennai 603 110, India, Tel. +91 9884823425; email: senthilchem8582@gmail.com*

Received 14 November 2015; Accepted 14 January 2016

ABSTRACT

The aim of the present investigation was to explore the performance of the acid-treated *Lantana camara* fruit biosorbent in binding hexavalent chromium from aqueous solutions. FTIR studies revealed the contribution of carbohydrates, glycosides, and flavonoids in the biosorbent. EDS analysis exhibited the occurrence of chromium ions after biosorption, whereas SEM image exposed the enhancement of porosity after acid treatment. The isotherm models such as Langmuir, Freundlich, Dubinin–Radushkevich, and Temkin models were studied to depict the mechanism of interaction of the biosorbent with the adsorbate. Besides isotherm models, kinetic studies like pseudo-first-order, pseudo-second-order, and intraparticle diffusion models were also performed to validate the controlling mechanism of biosorption. Langmuir model showed a better fit favoring monolayer adsorption and a high correlation value from the pseudo-second-order model suggests chemisorption. To understand whether the biosorption process releases or absorbs energy, thermodynamic analysis was carried out. The outcome of the findings showed endothermic nature of the process with increased randomness at the solid solution interface. Regeneration studies showed better results with 0.2 M NaOH solutions. The obtained maximum uptake capacity of 83 mg/g with a minimal biomass dosage proves the credible potential of the selected biosorbent in removing toxic hexavalent chromium.

Keywords: Lantana camara fruit; Chromium; Aqueous; Biosorbent; Acid

1. Introduction

In general, chromium ions exist in two oxidation states, namely, trivalent and hexavalent chromium. Naturally chromium is found as crocoite ($PbCrO_4$), chrome ochre (Cr_2O_3), and ferric chromite ($FeCr_2O_4$) deposits [1,2]. The anthropogenic sources are effluents from chromates, dichromates, dyes, varnishes, chromium–iron alloys processing units, and from electroplating, tannery, electronic, and metallurgy industries [3]. Superfund priority lists chromium as one of the top 20 contaminants and the most

*Corresponding author.

frequently occurring toxic metal for the past 15 years [4,5]. According to US Environmental Protection Agency, the maximum threshold limit for chromium in natural waters is 0.05 mg/L [6]. Acute exposure to hexavalent chromium causes diarrhea, nausea, liver and kidney damage, internal hemorrhage, and respiratory problems [7–9]. Moreover, hexavalent chromium is also considered as a potential carcinogen [10], whereas trivalent chromium is an essential micronutrient [11]. Chromium poses a serious health concern because of its oxidative capacity in forming free radicals and replacing these metals in enzymes interrupting their normal activity [12,13].

Conventional methods to remove chromium—ion exchange processes, precipitation techniques, oxidation/reduction systems, filtration processes, membrane technology, and evaporation processes—are extremely expensive and inefficient at lower metal ion concentrations. Moreover, they also add huge cost to the system with the generation of unwanted by-products which further needs effective treatment. This major limitation is overcome in the biosorption processes that work well even at a very low metal ion concentration. It is the process which uses dead biomass for removing heavy metals from the aquatic system [14]. It is also defined as the rapid and reversible binding process from aqueous solutions onto functional groups that are present on the biomass surface [15].

Various biosorbents like palm branches [8], tea extract [4], brown seaweed [16], citrus reticulate waste [17], pistachio hull waste [18], opuntia biomasss [19], coconut coir pith [20], lignite [21], chitosan [10], *Caryota urens* inflorescence waste biomass [22], etc., were investigated by other researchers to study the removal of hexavalent chromium by biosorption process. Pretreatments can also be used to enhance the metal uptake capacity which could be either heat treatment [23], or opening up of active sites for biosorption by acid treatment [24]. The present study uses acid pretreatment to improve the surface property of the biosorbent.

The plant *Lantana camara* with a small black colored fruit of 5 mm diameter persists throughout central and southern India in most dry stony hills and black soil [25]. This plant being an invasive species is considered as a biggest threat in Mudumalai Tiger Reserve. Hence, the fruit of this plant was collected in and around the Reserve and investigated for the biosorption of hexavalent chromium. The objective of the present study was to determine the maximum metal uptake capacity of the selected biosorbent. The performance of the raw and the pretreated biosorbent was compared by investigating on the selected operating parameters (pH, biomass dosage, contact time, temperature, and initial chromium ion concentration) pertaining to the biosorption of chromium. To understand the binding mechanism and nature of the biosorption process, isotherm, kinetic, and thermodynamic studies were carried out. Simultaneously desorption studies were also conducted using NaOH to ensure the reusability of the biosorbent.

2. Materials and methods

2.1. Biosorbent preparation

The *L. camara* fruits were collected from Masinagudi, Nilgris, Tamil Nadu, India. The fruits were washed with tap water to remove sand, dirt, and other impurities, and dried in hot air oven at 80˚C for 24 h. The fruits were then crushed in the domestic blender and sieved to obtain uniform particle size of 150 μm. They were also filtered by washing with distilled water using Buchner funnel under vacuum conditions to reduce the possibility of color leaching from the biosorbent into the aqueous Cr(VI) solution. The washing was carried out until the filtrate become colorless. Once again they were put in hot air oven at about 80˚C for 10 h. This raw biosorbent without any chemical activation was labeled as LC1 biosorbent which was stored in a dessicator for carrying out further experiments. Pretreatment of biosorbents was carried out for the enhancement of adsorption property [16,24,26]. The obtained LC1 biosorbent was treated with concentrated sulfuric acid (97%) in a ratio 1:1 for about 24 h. Later the residual acids were removed by washing the mixture with distilled water using Buchner funnel under vacuum. The resulting mixture was then dried in a hot air oven at a temperature of about 80˚C for 10 h, followed by subsequent grinding to a particle size of 150 μm . This chemically treated biosorbent was labeled as LC2 biosorbent which was also stored in the dessicator for performing further experiments.

2.2. Batch experimental studies

A 1,000 mg/L stock solution of Cr(VI) was prepared by dissolving 2.8287 g of potassium dichromate in 1,000 mL distilled water. A series of dilutions were done from the stock solutions to obtain 50, 150, 200, 250, 300, 350, 400, 450, and 500 mg/L sample solutions. The biosorption of hexavalent chromium on LC1 and LC2 was investigated by varying significant batch level parameters. The effects of initial chromium ion concentration (50–500 mg/L), biosorbent loading (0.05–0.9 g), pH (1–6), contact time (5–75 min), and temperature (303, 313, 323, and 333 K) on the

biosorption were studied. To study the biosorption isotherms, the optimum dose was fixed to be 0.2 g at the optimal pH of 1 and equilibrium time of 75 min for initial Cr(VI) ion concentrations ranging from 200 to 500 mg/L. Whereas, the kinetic study was performed for 100 mg/L initial chromium concentration at optimal conditions. Except thermodynamic study, all experiments were done at a temperature of 303 K. The volume of the adsorbate was maintained at 50 mL in 250 mL Erlenmeyer flask. The agitation speed was permanently fixed to be 160 rpm in the orbital incubator shaker (SLM-INC-OS-250). The separation of biosorbent from the adsorbate was done using Whatman filter paper (no. 41). The pH modifications of the aqueous Cr(VI) solution were accomplished by digital pH meter (systronic) using 0.1 N HCl. The analysis for final Cr(VI) ions after biosorption process was determined in a Shimadzu UV–vis spectrophotometer at a wavelength of 540 nm. This was done after the formation of Cr(VI)—DPC complex with the addition of 1, 5 diphenylcarbazide. The Cr(VI) uptake capacity of the biosorbent at equilibrium condition was calculated using the following Eq. (1):

$$q_e = \frac{(C_0 - C_e)V}{m} \quad (1)$$

where q_e is the equilibrium biosorption capacity (mg/g), C_0 and C_e are the initial and equilibrium Cr(VI) concentrations (mg/L), respectively, m is the biosorbent dosage (g), and V is the volume of the adsorbate (L).

2.3. Biosorbent characterization

To determine the functional groups present in the biosorbent, an infra-red spectrum analysis was performed using FTIR spectrophotometer (Nicolet IS 10, USA) in the wavelength range from 4,000 to 400 cm^{-1}. This analysis was carried out to determine the native functional groups present in the raw biosorbent and to study its influence on adsorption. In addition to this, the analysis was also extended to the LC2 biosorbent and chromium-loaded LC2 biosorbent. The morphological changes of the biosorbent before and after the biosorption process were explored using scanning electron microscope (SEM-Carl Zeiss, Sigma version). Furthermore, energy-dispersive X-ray spectroscopy was used to determine the occurrence of Cr(VI) ions on the surface of biosorbent after biosorption.

2.4. Biosorbent desorption

The effective utilization of the selected biosorbent will be guaranteed only on exploring the reusability of the selected biosorbent. Hence, the study of desorption plays a vital role in the biosorption processes for removing any metals. Biosorption and desorption processes were done in cycles up to five times, using 0.2 N NaOH as a desorbing agent. At the end of each cycle the biosorbents were washed with distilled water and used for the next biosorption cycle. The chromium-loaded biomass (50 mg/L) was contacted with 0.2 N NaOH at a temperature of 303 K. They were shaken for about 75 min at 160 rpm in the orbital incubator shaker. The separated biosorbents were washed and used as described above.

3. Results and discussions

3.1. Biosorbent characterization

The different band positions from the FTIR spectra of the raw biosorbent before biosorption (Fig. 1(a)) are shown in Table 1. The peak around 1,060 cm^{-1} was attributed as a characteristic peak for C–O stretching in carbohydrates. Further, the presence of flavonoids was confirmed by the appearance of a peak around 1,641 cm^{-1} holding C=O stretch. In addition to the 1,421 cm^{-1} band, the presence of carboxylic acids was also confirmed by the strong and broad band for OH stretch at 3,400 cm^{-1}. The weak band at 2,936 cm^{-1} matches to the CH stretching vibration and 1,518 cm^{-1} refers to the benzene ring present in flavonoids and glycosides. The weak band at 1,259 cm^{-1} could be attributed to C–O stretching vibration. The results of the LC2 biosorbent after acid treatment continue to show all the predominant functional groups for *L. camara* fruit with some marginal changes in vibrational frequencies. Hence, FTIR results reveal the presence of carbohydrates, glycosides, and flavonoids in the selected biosorbent.

On comparing the unloaded biosorbent (Fig. 1(b)) with metal-loaded biosorbent for LC2 spectra (Fig. 1(c)), vibrational frequencies exhibited significant differences as shown in Table 2. A remarkable shift is observed in the peak 2,879 and 2,822 cm^{-1} which is assigned to CH stretching vibration. A notable difference in the peak is also observed in 1,515 cm^{-1} indicating the distortion in the benzene ring. The changes are also dominant for carboxylic acid group in 1,400 cm^{-1} band and hydroxyl group in 3,414 cm^{-1}. Hence it is confirmed that the hydroxyl, carboxyl, and aliphatic CH groups present in the biosorbent help in the biosorption of hexavalent chromium. Hence, the change in bands at 3,414 cm^{-1} (O–H) and 2,879 cm^{-1} (C–H) implies the dominant complexation process [18,27] involving electrostatic attraction between the anionic chromium and the

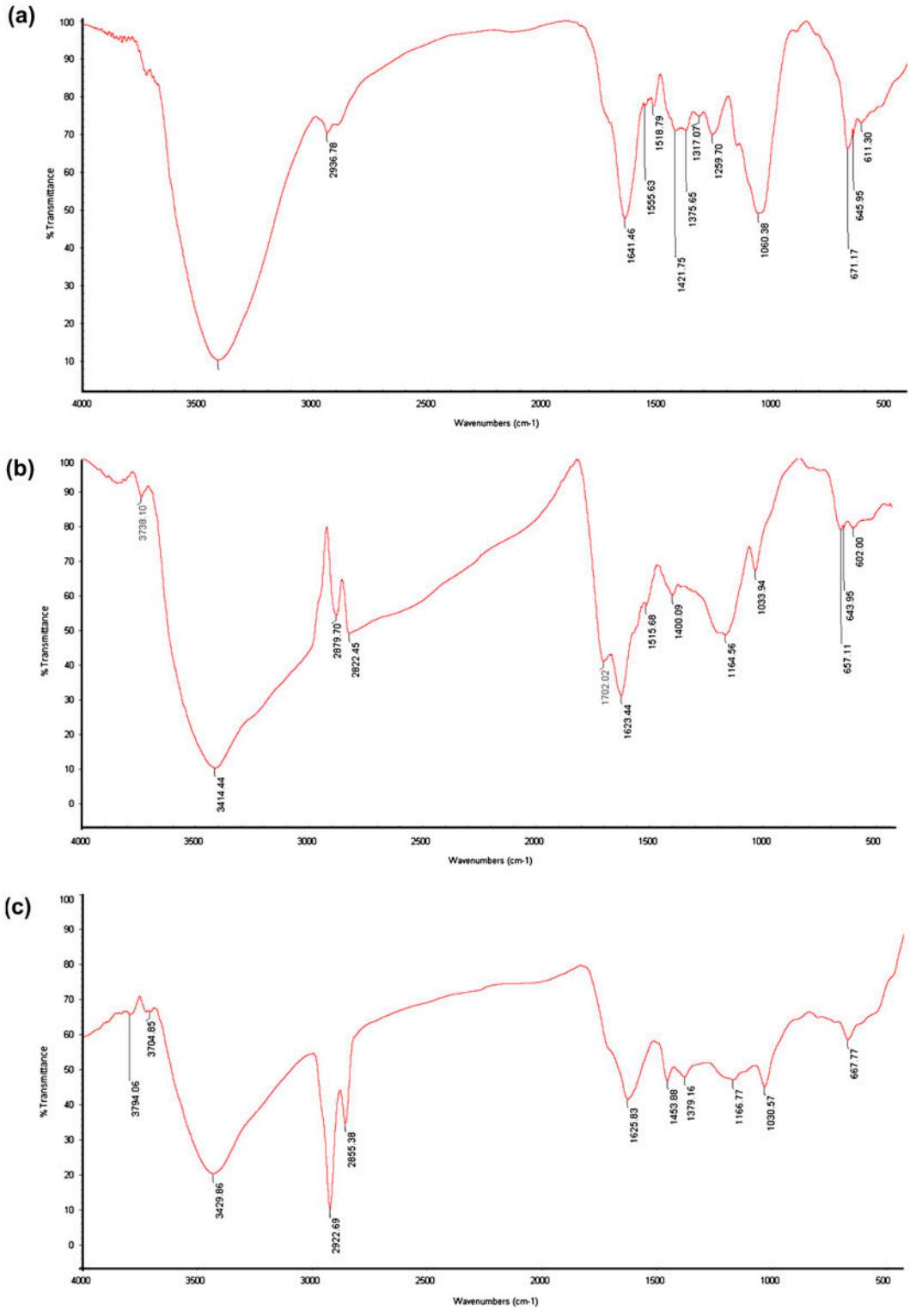

Fig. 1. FTIR spectra of (a) LC1 biosorbent, (b) LC2 biosorbent, and (c) Cr(VI)-loaded LC2 biosorbent.

Table 1
FTIR for raw biosorbent before biosorption

Band position (cm)	Functional groups
3,400	OH group
2,936	Aliphatic CH stretching vibration
1,641	C=O stretch
1,421	O–C=O linkage
1,518	Benzene ring in aromatic compounds
1,259	C–O stretching vibration
1,060	C–O stretching vibration
671	C–H bending

aforesaid functional groups on the biosorbent surfaces. Fig. 2(a) and (b) represents the scanning electron micrograph of the raw and chromium-loaded biomass for LC1. Fig. 2(c) and (d) represents the image of the raw and chromium-loaded biomass for LC2. Even without any chemical modification, LC1 still possesses a porous structure showing a potential for biosorption of metals. Later after biosorption the pores were completely absent, indicating the possibility of binding chromium ions. After acid treatment, the biosorbent was characterized by an uneven porous structure as shown in Fig. 2(c). Whereas after biosorption, macro porous structure of the biosorbent created and the voids occupied by the chromium ions confirm the likelihood for the diffusion of these metal ions into the biosorbent. The EDX spectrum image for LC1 and LC2 biosorbent before and after biosorption is given in Fig. 3(a)–(d). The distinct peaks in Fig. 3(b) and (d) show the presence of hexavalent chromium for both the biosorbents. This phenomenon validates the biosorption of hexavalent chromium ions onto the selected biosorbents.

3.2. Effect of pH

The role of pH is one of the significant factors in governing the biosorption of hexavalent chromium. The effect of pH on the enhancement of adsorption capacity was studied between 1 and 6 and the results were interpreted as shown in Fig. 4. This study is done for a 400 mg/L chromium concentration solution for the dosage of 0.5 g equilibrated at 75 min. The adsorption capacity decreases with increase in pH from 1 to 6 with an effective adsorption capacity at a lower pH of 1. The same trend is observed for both the studied biosorbents. Favorable results were obtained at a pH of 1 with 34 and 40 mg/g adsorption capacities for LC1 and LC2 biosorbents, respectively. This increased uptake capacity at acidic pH range is due to increased electrostatic attraction and binding of negatively charged hexavalent chromium species onto the positively charged surface of the LC1 and LC2 biosorbent [20,28]. The various forms of hexavalent chromium in aqueous solution are $Cr_2O_7^{2-}$, CrO_4^{2-}, and $HCrO_4^-$. Cr(VI) is present in $HCrO_4^-$ form at a pH between 1 and 4 and then changes to CrO_4^{2-} form with increase in pH which is basically a divalent form [29]. At a lower pH of 1, $HCrO_4^-$ oxyanions strongly interact with the positive surfaces of the LC1 and LC2 biosorbents [30]. Hence this active participation of carboxyl and hydroxyl functional groups in the biosorbent is influenced based only on the pH value of the aqueous solution. At higher pH values building up of negative charges on the biosorbent causes electrostatic repulsion and decreases the possibility for biosorption of chromium ions. Henceforth it is concluded that the enhanced biosorption is mainly because of the chemical interactions between the protonated biosorption sites and negatively charged sorbate

Table 2
FTIR for activated biosorbent before and after biosorption

Band position (cm)			
Before biosorption	After biosorption	Differences	Functional groups
3,414	3,429	15	OH group
2,879	2,922	43	Aliphatic CH stretching vibration
2,822	2,855	33	Aliphatic CH stretching vibration
1,623	1,625	2	C=O stretch
1,515	1,453	62	Benzene ring in aromatic compounds
1,400	1,379	21	O–C=O linkage
1,164	1,166	2	C–O stretching vibration
1,033	1,030	3	C–OH stretching vibration
602	667	65	C–H bending

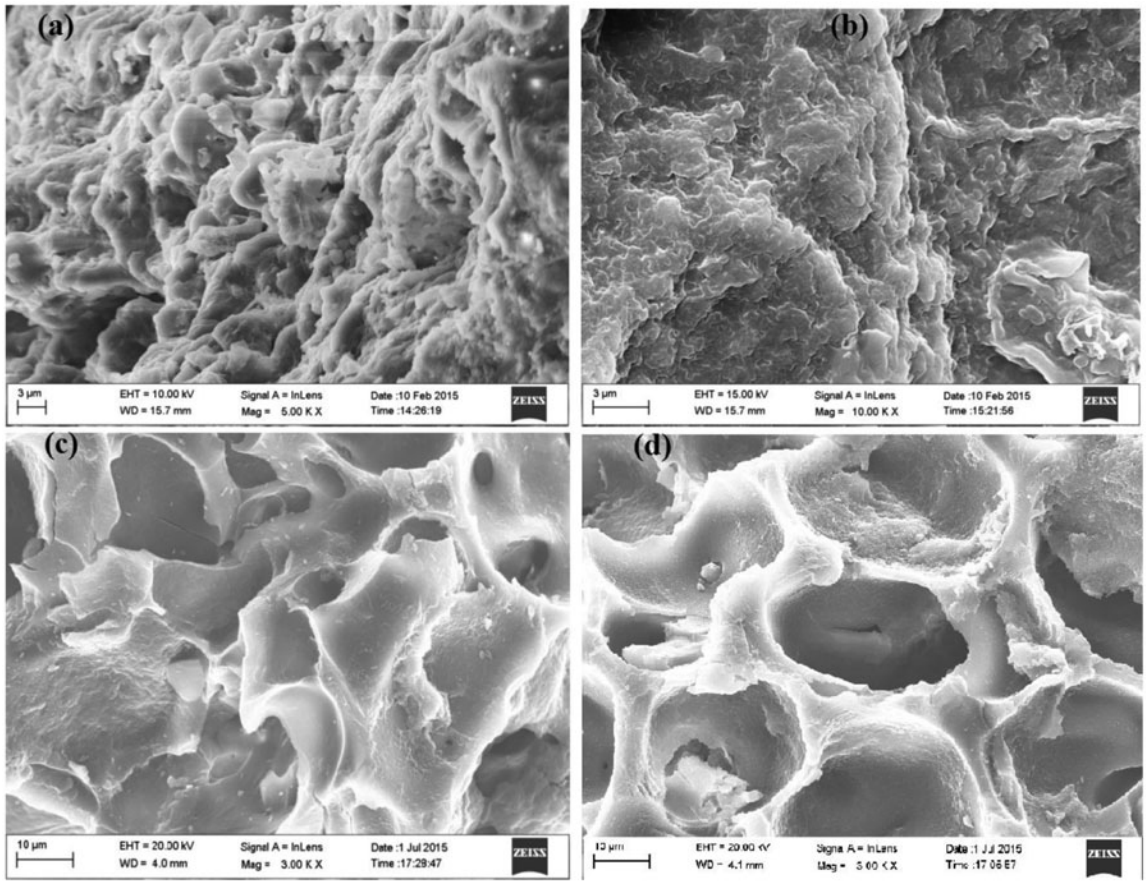

Fig. 2. Scanning electron micrograph pictures of (a) LC1 before Cr(VI) biosorption, (b) LC1 after Cr(VI) biosorption, (c) LC2 before Cr(VI) biosorption, and (d) LC2 after Cr(VI) biosorption.

[19,31]. Based on these findings the optimum pH for the rest of the experiments was fixed to be 1.0.

3.3. Effect of biosorbent dosage

The value of the biosorbent dosage is directly involved in the calculation of the metal uptake capacity of the biosorbent. Moreover, optimizing this parameter also reduces the overall treatment cost in the biosorption process. The study on biosorbent dosage (0.05–0.09 g) was carried out for 400 mg/L chromium concentration at a pH value of 1. The effect of biosorption on metal uptake capacity and the removal efficiency entirely shows an opposite trend. Fig. 5 exhibits the decrease in uptake capacity with increase in biomass dosage and Fig. 6 depicts the increase in adsorption efficiency followed by saturation. This increase in biosorption efficiency is due to added active sites for the same amount of metal ions in the solution and saturation is because of the aggregation of solid particles at higher loadings [18]. In order to obtain 99% removal efficiency, 0.9 g of LC1 biosorbent is required, whereas the same removal efficiency is obtained with only 0.55 g for LC2 biosorbent. The maximum adsorption capacity was found to be 120 mg/g at a minimum dosage of 0.05 g for LC2 biosorbent which was found to be quite higher than obtained for LC1 biosorbent (88 mg/g). This increase in biosorption is because of the more number of active sites at higher dosages. However, the increase was also followed by a saturation stage at very high dose levels which is because of the solid particle agglomeration. This further limits the surface area available for binding of chromium ions [18].

3.4. Effect of contact time

To design a continuous adsorption system, predicting the rate of reaction plays a major role in understanding the feasibility of the process [32]. If the saturation time is attained in a very short span of time, this system could be very easily adapted for the

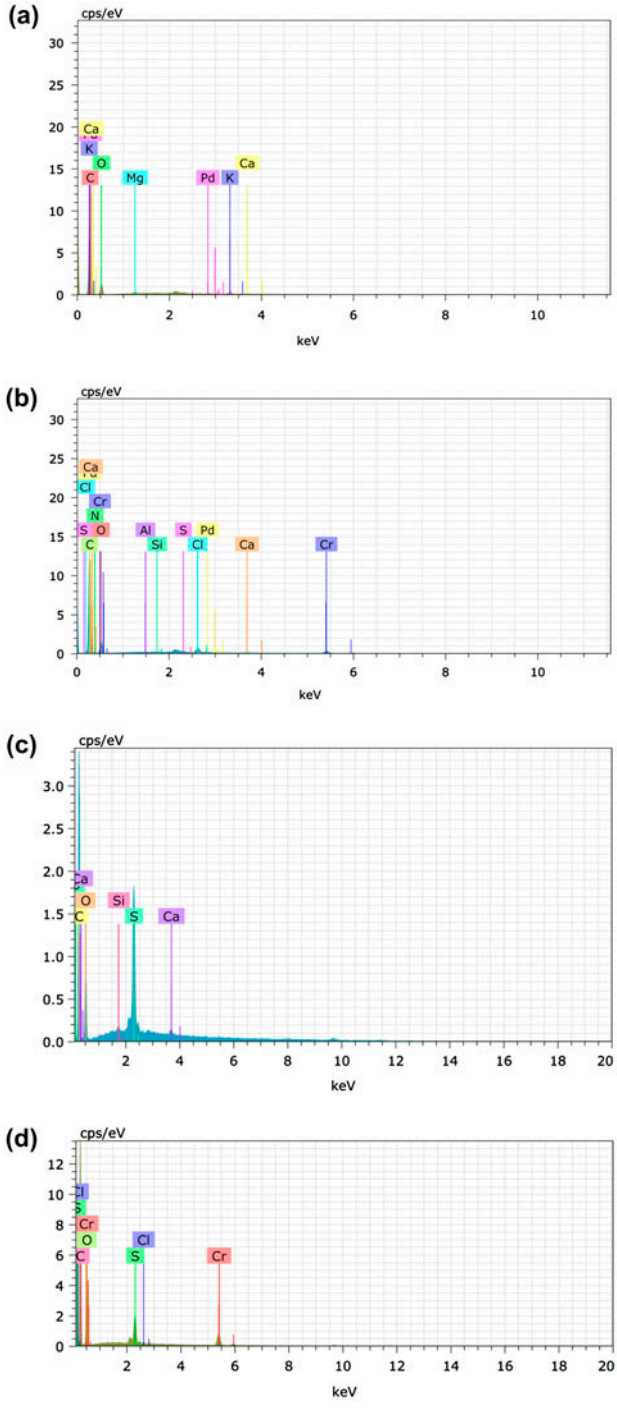

Fig. 3. EDS picture of micrographs of (a) LC1 before Cr (VI) biosorption, (b) LC1 after Cr(VI) biosorption, (c) LC2 before Cr(VI) biosorption, and (d) LC2 after Cr(VI) biosorption.

large-scale continuous system. Hence, the effect of contact time on biosorption efficiency was investigated for 400 mg/L initial chromium concentration. The pH

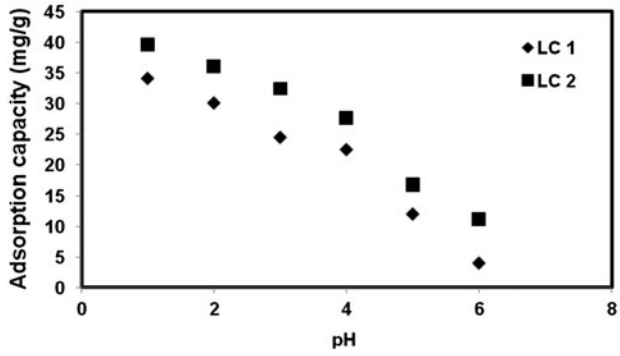

Fig. 4. Effect of pH of aqueous Cr(VI) on the adsorption capacity of the LC1 and LC2 biosorbent.

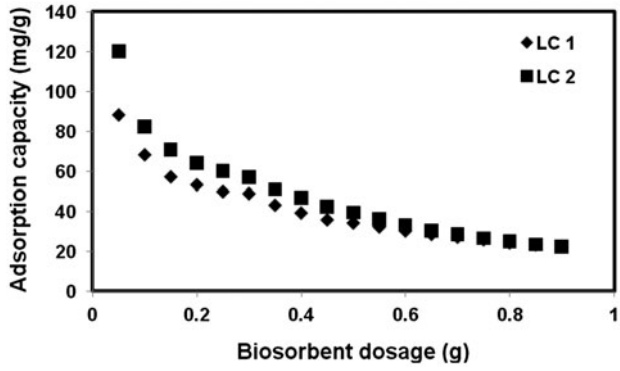

Fig. 5. Effect of biosorbent dosage on the adsorption capacity of the LC1 and LC2 biosorbent.

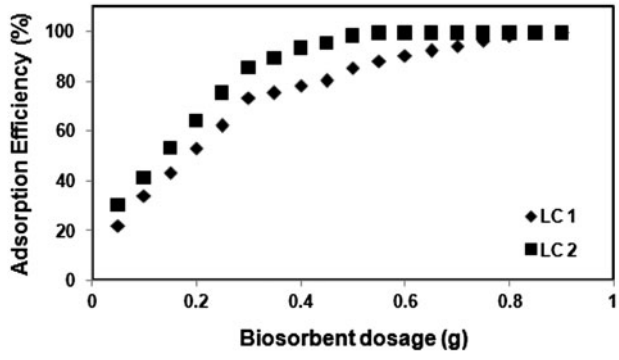

Fig. 6. Effect of biosorbent dosage on Cr(VI) removal efficiency on the LC1 and LC2 biosorbent.

was maintained to be 1 at a dosage level of 0.5 g of the biosorbent. The performance of the LC1 biosorbent was compared with the LC2 biosorbent as shown in Fig. 7.

The metal uptake capacity was calculated for every five minutes interval until the attainment of

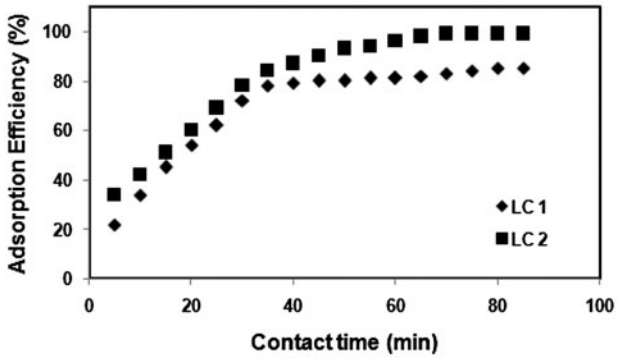

Fig. 7. Effect of contact time on chromium(VI) removal efficiency on the LC1 and LC2 biosorbent.

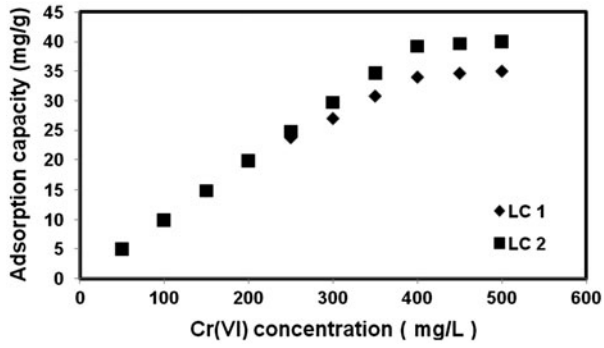

Fig. 8. Effect of initial Cr(VI) ions concentration on adsorption capacity of LC1 and LC2 biosorbent.

equilibrium. The adsorption efficiency increased rapidly in the beginning, followed by a slower phase approaching equilibrium condition. The equilibrium time was found to be the same for both the biosorbents, which was found to be 75 min. But the maximum adsorption efficiency varied and was found to be 85 and 99% for LC1 and LC2 biosorbents, respectively. In the beginning of biosorption, availability of more number of active binding sites of the biosorbent and larger surface area facilitates the binding of Cr(VI) ions, which may ultimately lead to faster adsorption. Slower phase in the later stage may be because of the occupation of active adsorption sites by the Cr(VI) ions and may also involve other principles like microprecipitation, complexation [33], and intraparticle diffusion [17,34].

3.5. Effect of initial Cr(VI) ion concentration

This study was done for different initial chromium concentrations ranging from 50 to 500 mg/L at a pH value of 1. The adsorption capacity increases with increase in the chromium concentration, whereas the efficiency shows a decreasing trend (figure not shown). This is because the active binding sites of biosorbent are not plentiful to bind larger concentration of chromium ions, which could be easily possible in lower Cr(VI) ions concentration. As the optimum dosage was fixed to be 0.5 g, both the biosorbents exhibited the same adsorption efficiency and uptake capacity up to 200 mg/L. But beyond this value the adsorption capacity showed different values and saturated at a concentration of 400 mg/L as shown in Fig. 8.

The maximum adsorption capacity was calculated to be 35 and 40 mg/g at a concentration of 500 mg/L for LC1 and LC2, respectively. The enhanced uptake capacity at higher concentrations may be due to the significant interaction between the biosorbent and the adsorbate. Furthermore, larger concentrations also create enough driving force to manage the mass transfer resistance between the LC biosorbent and Cr(VI) ions present in the solution.

3.6. Effect of temperature

The effect of temperature on biosorption of chromium ions was studied for temperatures ranging from 303 to 333 K at a pH of 1 with 400 mg/L as initial metal ion concentration. The biosorption showed better removal efficiency with increase in temperature for the studied concentration. The removal percentage increased from 85 to 96% and 98 to 99% for LC1 and LC2 biosorbents, respectively, as shown in Fig. 9. The enhanced removal efficiency and better biosorption capacity with increase in temperature reveals the nature of the process to be endothermic.

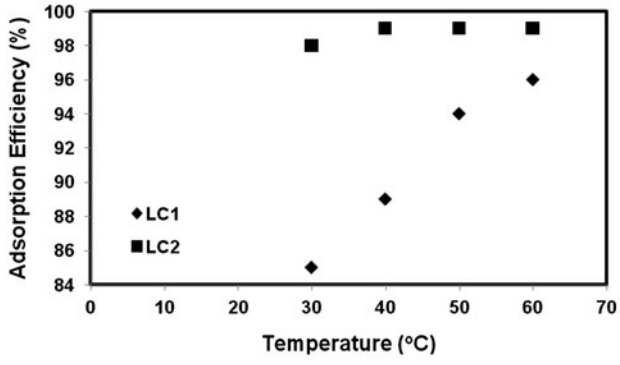

Fig. 9. Effect of temperature on Cr(VI) removal efficiency using LC1 and LC2 biosorbent.

Table 3
Langmuir separation factor (R_L) for LC1 and LC2 biosorbents

Type of biosorbent	Separation factor (R_L) based on Langmuir model Initial Cr(VI) ions concentration (mg/L)						
	200	250	300	350	400	450	500
LC1	0.2	0.16	0.14	0.13	0.11	0.10	0.09
LC2	0.16	0.14	0.12	0.10	0.09	0.08	0.07

3.7. Isotherm studies

3.7.1. Langmuir model

The Langmuir adsorption isotherm [35,36] is given by the following Eq. (2), which defines monolayer coverage of adsorbate on the homogeneous biosorbent surface [22,37]:

$$\frac{1}{q_e} = \frac{1}{q_{max} b C_e} + \frac{1}{q_{max}} \quad (2)$$

In this model, q_{max} (mg/g) is the amount of adsorption corresponding to complete monolayer coverage, i.e. the maximum adsorption capacity and b (L/mg) is the Langmuir constant. To determine whether the adsorption process is favorable or not in Langmuir-type adsorption processes, a dimensionless separation factor R_L is used which is given as in Eq. (3) [38,39]:

$$R_L = \frac{1}{1 + bC_0} \quad (3)$$

If $R_L > 1$, the isotherm is unfavorable; $R_L = 1$, the isotherm is linear; $0 < R_L < 1$, the isotherm is favorable; $R_L = 0$, the isotherm is irreversible. The separation factor values as obtained in Table 3, which are found in the range of 0–1 indicate that the biosorption is favorable in removing Cr(VI) ions using both LC1 and LC2 biosorbents.

Favorable adsorption was also supported with the linear plot of $1/q_e$ vs. $1/C_e$ (Figs. 10 and 11) which shows a better fit with a high R^2 values for both the biosorbents. This indicates the applicability of monolayer adsorption with maximum monolayer adsorption capacity values of 66 and 83 mg/g, respectively, for LC1 and LC2 biosorbents as shown in Table 4. It also shows a lower Langmuir constant values of 0.020 and 0.025 L/mg showing higher viability for Cr(VI) ions to adsorb onto the selected biosorbents.

3.7.2. Freundlich adsorption model

The Freundlich model defines a better fit for adsorption of liquids which is expressed as (Eq. (4)):

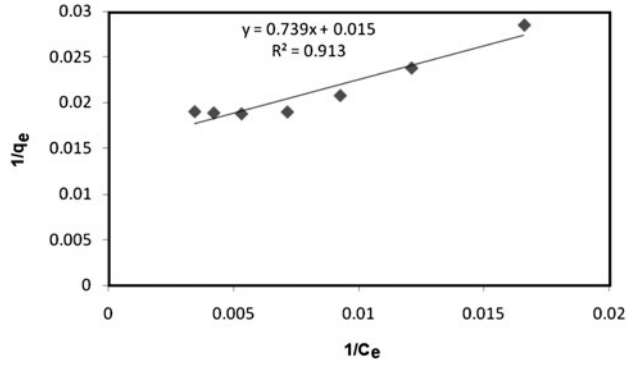

Fig. 10. Langmuir isotherm plot for the biosorption of Cr (VI) on LC1 biosorbent.

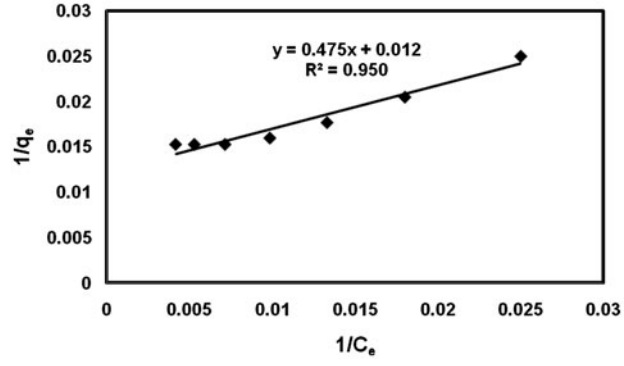

Fig. 11. Langmuir isotherm plot for the biosorption of Cr (VI) on LC2 biosorbent.

$$\log q_e = (1/n) \log C_e + \log K_F \quad (4)$$

In this model, the mechanism and the rate of adsorption are functions of the constants $1/n$ and K_F (L/g). The Freundlich isotherm is mainly applicable for heterogeneous surface adsorption. This model assumes that the binding sites which are stronger are occupied first and later the binding strength decreases upon occupation of these active sites [40,41].

The slope between 0 and 1 is a measure of adsorption intensity or surface heterogeneity, and the

Table 4
Parameters derived from different isotherm studies for the biosorption of Cr(VI) on LC1 and LC2 biosorbent

Type of biosorbent	Langmuir isotherm	Freundlich isotherm	Temkin model	Dubinin–Radushkevich model
LC1	q_{max} = 66 mg/g b = 0.020 L/mg R^2 = 0.91	K = 14.02 mg/g n = 4.048 R^2 = 0.78	A = 0.567 l/mg B = 0.20 kJ/mol R^2 = 0.80	q_{max} = 45.69 mg/g E = 0.1 kJ/mol $K_{DR} = 3 \times 10^{-6}$ mol^2/J^2 R^2 = 0.62
LC2	q_{max} = 83 mg/g b = 0.025 L/mg R^2 = 0.95	K = 17.02 mg/g n = 3.846 R^2 = 0.82	A = 0.608 l/mg B = 0.18 kJ/mol R^2 = 0.86	$q_{m,D}$ = 52.77 mg/g E = 0.4 kJ/mol $K_{DR} = 3 \times 10^{-5}$ mol^2/J^2 R^2 = 0.52

process becomes more and more heterogeneous as it is approaching zero. A value of $1/n$ less than 1 implies chemisorptions process and if it is greater than one, it indicates cooperative adsorption [42,43]. Henceforth, based on the results given in Table 4, the Freundlich constant $1/n$ less than 1 confirms the indication of chemical adsorption. However, the coefficient of determination values calculated from the log q_e vs. log C_e plot (Figs. 12 and 13) does not represent a best fit to the experimental data for both the biosorbents. Hence, the applicability of heterogeneous adsorption becomes less valid for the selected biosorbents.

3.7.3. Temkin isotherm model

Temkin's model is not applied under extremely low and high concentrations [44,45]. This model is based on the assumption that the free energy of sorption is a function of the surface coverage and also accounts for the interactions between adsorbents and metal ions to be biosorbed [40,41,46,47].

The Temkin isotherm [48] is expressed as follows (Eq. (5)):

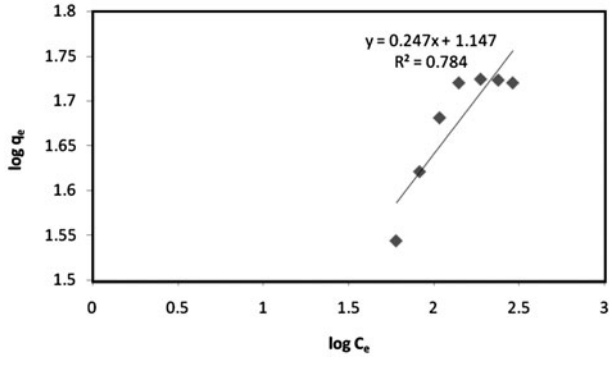

Fig. 12. Freundlich isotherm plot for the biosorption of Cr (VI) on LC1 biosorbent.

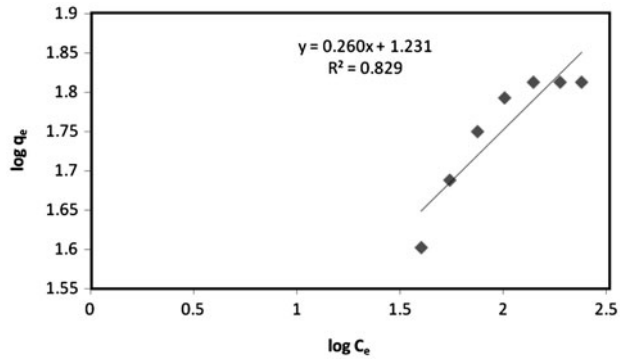

Fig. 13. Freundlich isotherm plot for the biosorption of Cr (VI) on LC2 biosorbent.

$$q_e = \frac{RT}{b} \ln(AC_e) \tag{5}$$

A linear form of the Temkin isotherm can be expressed as (Eqs. (6) and (7)):

$$q_e = \frac{RT}{b} \ln A + \frac{RT}{b} \ln C_e \tag{6}$$

$$q_e = B \ln A + B \ln C_e \tag{7}$$

where $B = RT/b$, R is the gas constant (8.314 J/mol/K), T is the temperature (K). Based on the plot of q_e vs. ln C_e as shown in Figs. 14 and 15, the constants A and B are determined.

These are found to be 0.567 l/mg and 0.20 kJ/mol for LC1 biosorbent and 0.608 l/mg and 0.18 kJ/mol for LC2 biosorbent, respectively. Though Temkin isotherm exhibits a correlation value of 0.80 and 0.86 (Table 4) for both the biosorbents, the validity was found to be less when comparing it with Langmuir isotherm. This proves that surface interaction is not

the dominant factor behind the biosorption of Cr(VI) ions onto the surface of the biosorbent and hence the likelihood of this mechanism is only less possible.

3.7.4. Dubinin–Radushkevich model

The Dubinin–Radushkevich isotherm is used to interpret the biosorption mechanism with a Gaussian energy distribution onto a heterogeneous surface [49,50]. The Dubinin–Radushkevich adsorption isotherm is expressed as (Eq. (8)):

$$q_e = q_{m,D} \exp(-K_{DR}\varepsilon^2) \quad (8)$$

The parameter ε can be found from Eq. (9):

$$\varepsilon = RT \ln\left[1 + \frac{1}{C_e}\right] \quad (9)$$

where $q_{m,D}$ is the maximum amount of Cr(VI) uptake on biosorbent (mg/g), ε is the Polanyi potential of Dubinin–Radushkevich model, R is the gas constant (8.314 J/mol/K), T is the absolute temperature, and K_{DR} is the Dubinin–Radushkevich constant. E is the mean biosorption energy of biosorption which can be calculated using the Eq. (10).

$$E = 1/\sqrt{2K_{DR}} \quad (10)$$

Mean biosorption energy value gives significant information on predicting the type of biosorption process. If $E < 8$ kJ/mol, the biosorption process is defined as physisorption process. If $E > 16$ kJ/mol, chemisorption is the dominating factor. If E lies between 8 and 16 kJ/mol, biosorption process might be due to exchange of ions [22]. As shown in Table 4, E value

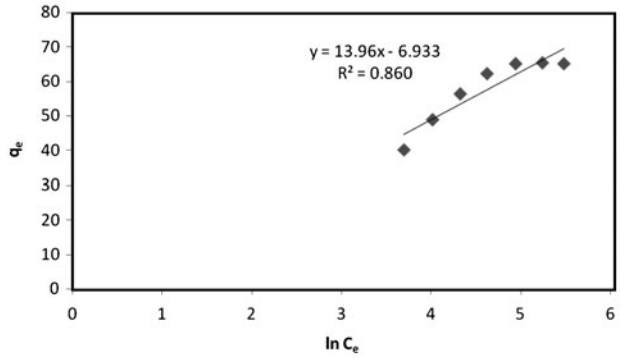

Fig. 15. Temkin isotherm plot for the biosorption of Cr(VI) on LC2 biosorbent.

<8 kJ/mol, both the biosorbents communicate the fact that the biosorption follows physisorption. However, a very less correlation value was obtained than other studied models ($R^2 < 0.65$) (Figs. 16 and 17) both the biosorbents suggest that this model is invalid and not appropriate for the present study. In addition, the maximum uptake capacity as shown in the table is also far-off from the experimental values (Table 5).

3.8. Biosorption kinetics

To understand the controlling mechanism for biosorption, kinetic models, namely pseudo-first-order, pseudo-second-order, and intraparticle diffusion models, were investigated. Specifically, intraparticle diffusion model was applied to understand whether boundary layer diffusion effect plays a predominant role in the biosorption of Cr(VI) ions. Whereas pseudo-first- and -second-order models compare the experimental adsorption capacity with the calculated values.

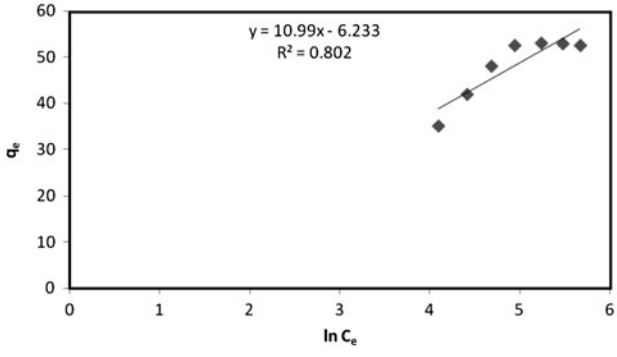

Fig. 14. Temkin isotherm plot for the biosorption of Cr(VI) on LC1 biosorbent.

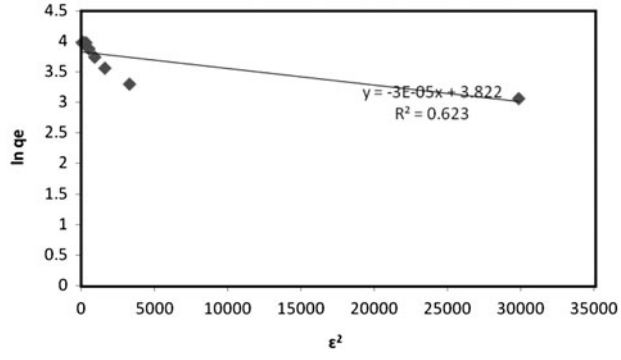

Fig. 16. Plot for Dubinin–Radushkevich model for the biosorption of Cr(VI) on LC1 biosorbent.

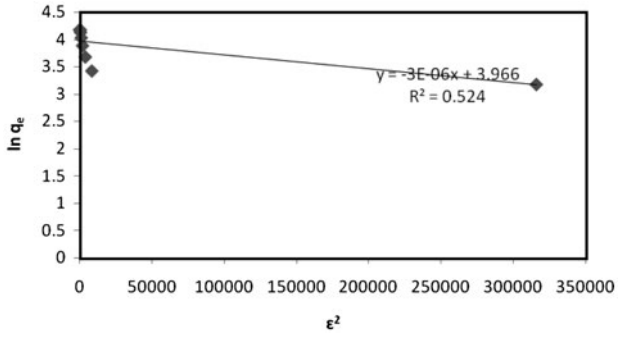

Fig. 17. Plot for Dubinin–Radushkevich model for the biosorption of Cr(VI) on LC2 biosorbent.

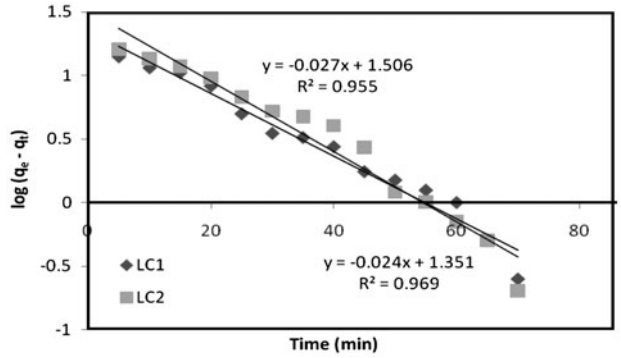

Fig. 18. Pseudo-first-order plot for the biosorption of Cr (VI) on LC1 and LC2 biosorbents.

3.8.1. The pseudo-first-order and -second-order kinetic model

Pseudo-first-order model assumes that the rate of occupation of biosorption sites is proportional to the number of unoccupied sites. The linear pseudo-first-order equation [51] is given as follows (Eq. (11)):

$$\log(q_e - q_t) = \log q_e - \frac{k_1 t}{2.303} \tag{11}$$

where q_t and q_e represents the Cr(VI) adsorbed at time t and at equilibrium (mg/g), respectively, and k_1 is the rate constant of pseudo-first-order adsorption process (min^{-1}). Based on the slope and intercept obtained from the straight line plot of $\log(q_e - q_t)$ vs. t (Fig. 18) the values of pseudo-first-order rate constants k_1, and equilibrium biosorption capacities q_e are calculated.

The kinetic data were further studied [52] using Ho's pseudo-second-order kinetic model. This model assumes that the biosorption follows second-order chemisorption. It can be expressed as (Eq. (12)):

$$\frac{dq_t}{dt} = k(q_e - q_t)^2 \tag{12}$$

Integrating Eq. (12) and applying the boundary conditions, gives (Eq. (13)):

$$\left(\frac{1}{q_e - q_t}\right) = \frac{1}{q_e} + kt \tag{13}$$

Eq. (13) can be rearranged to obtain a linear form (Eq. (14)):

$$\frac{t}{q_t} = \frac{1}{h} + \frac{1}{q_e} t \tag{14}$$

where $h = kq_e^2$ (mg/g/min) can be regarded as the initial adsorption rate as $t \rightarrow 0$ and k is the rate constant of pseudo-second-order adsorption (g/mg/min). Based on the plot of t/q_t vs. t q_e, k and h were determined from the slope and intercept of the plot, respectively (Fig. 19).

Table 5
Comparison of the maximum biosorption capacity of various acid pretreated biosorbents on removing Cr(VI) ions

Acid pretreated biosorbent	Pretreated acid	q_{max} (mg/g)	Refs.
Water lily (aquatic weeds)	Sulfuric acid	8.4	[26]
Mangrove leaves	Sulfuric acid	8.8	[26]
Neurospora crassa (fungal biomass)	Acetic acid	16.0	[62]
Opuntia biomass	Sulfuric acid	18.5	[19]
Chlamydomonas reinhardtii (microalgae)	Hydrochloric acid	21.2	[23]
Oedogonium hatei (algal species)	Hydrochloric acid	35.2	[33]
Swietenia mahagoni (shells)	Sulfuric acid	47.6	[63]
Swietenia mahagoni (shells)	Orthophosphoric acid	58.8	[63]
Lantana camara	Sulfuric acid	83.0	Present study
Immobilized *Aspergillus niger* biomass (fungal species)	Sulfuric acid	92.5	[64]
Strychnos potatorum seeds	Sulfuric acid	202.7	[65]

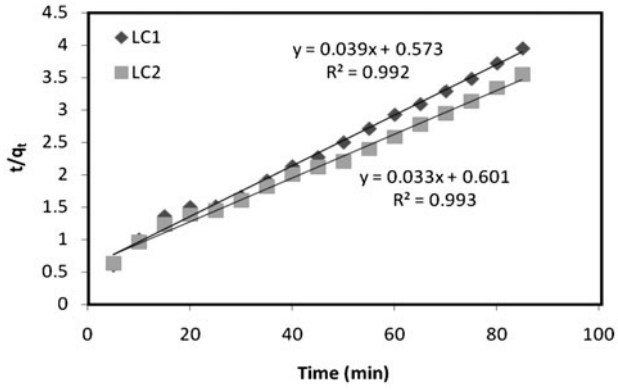

Fig. 19. Pseudo-second-order plot for the biosorption of Cr (VI) on LC1 and LC2 biosorbents.

Most of the kinetic studies done by various researchers consisted of two phases: an initially rapid phase followed by a slower phase as shown in Fig. 7 [53–55]. The initial rapid stage in the present study happened for the first 35 min followed by a slower phase up to 120 min. The results of the kinetic data for both pseudo-first- and -second-order models are tabulated as shown in Table 6. Despite the fact that both the models show high correlation values ($R^2 > 0.90$) for both LC1 and LC2 biosorbents, pseudo-second-order model shows the best fit with a very high correlation value of 0.99. Moreover, Table 6 also shows that the calculated adsorption capacity values are found to be almost close to the experimental values for both the models. But based on the coefficient of determination, it is concluded that the biosorption in the present study influences a pseudo-second-order model. This represents that biosorption is likely to be governed by chemisorption process [56], which includes the sharing or exchanging of electrons between metal ion and adsorbent. This also reveals the fact that both metal ion concentration and biosorbent dosage contributes to the biosorption of hexavalent chromium.

3.8.2. Intraparticle diffusion model

To study the diffusion mechanism, the intraparticle diffusion model was also tested [57,58]. The intraparticle diffusion equation is represented by (Eq. (15)):

$$q_t = k_{\text{ipd}} t^{1/2} + C_i \tag{15}$$

where k_{ipd} is the intraparticle diffusion rate constant (mg/g $\text{min}^{1/2}$), while C_i is the intercept at stage i. As the applicability of chemisorptions is confirmed for the present system, the validity of intraparticle diffusion model is also investigated to check the likelihood of external and internal diffusion effects on the biosorption of Cr(VI) ions. The plot of adsorption capacity against contact time square root is depicted in Fig. 20, which shows that the initial curved portions [33] could be attributed to the boundary layer diffusion effect [59], and the final linear portion might be due to intraparticle diffusion process [60] which is followed by a plateau on attaining saturation. In addition, intraparticle diffusion is the only rate-limiting phenomena if the curve is linear and passes through the origin. But the curve obtained infers that it is neither completely linear nor passes through the origin.

This confirms that the biosorption of Cr(VI) ions is not restricted to intraparticle diffusion and is not the only rate-limiting factor, whereas boundary layer diffusion also plays a role to some extent, in the binding of hexavalent chromium ions. Boundary layer diffusion effect is also confirmed by a reasonably high intercept value as shown in Table 6. These phenomena are applicable to both LC1 and LC2 biosorbents as both have the correlation values between 0.80 and 0.85 and higher values for intercepts, which is presented in Table 6.

3.9. Thermodynamic studies

In order to determine the spontaneity and heat change in the biosorption of Cr(VI) [22,61],

Table 6
Parameters derived from different kinetic models for the biosorption of Cr(VI) on LC1 and LC2 biosorbent

	Parameters of kinetic models at 303 K for100 mg/L of Cr(VI) ions concentration									
	Pseudo-first-order model			Pseudo-second-order model			Intraparticle diffusion model			Experimental
Biosorbent	R^2	k_1 (min)	$q_{e(cal)}$ (mg/g)	R^2	k (g/mg/min)	$q_{e(cal)}$ (mg/g)	R^2	k_{ipd} (mg/g/$\text{min}^{1/2}$)	C_i (mg/g)	$q_{e(exp)}$ (mg/g)
LC1	0.96	0.055	22.43	0.99	0.0026	25.64	0.81	0.319	10.48	21
LC2	0.95	0.062	32.06	0.99	0.0018	30.30	0.85	0.380	10.87	24

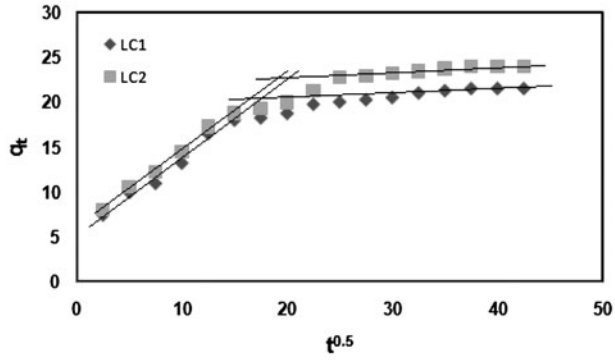

Fig. 20. Intraparticle diffusion plot for the biosorption of Cr(VI) on LC1 and LC2 biosorbents.

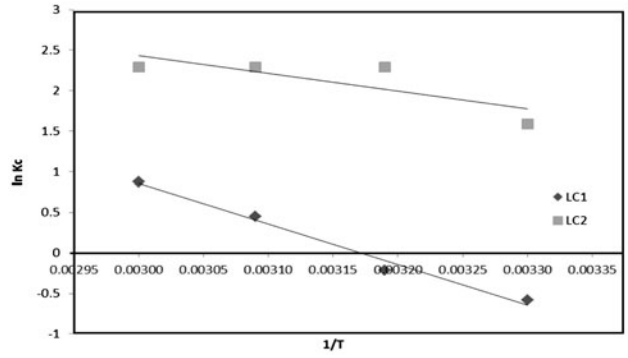

Fig. 21. Thermodynamic plot for the biosorption of Cr(VI) on LC1 and LC2 biosorbents.

thermodynamic parameters, including the change in free energy (ΔG°), enthalpy (ΔH°), and entropy (ΔS°) were calculated from the following equations (Eqs. (16) and (17)):

$$\Delta G^{\circ} = -RT \ln K_C \tag{16}$$

$$\ln K_C = \frac{-\Delta H^{\circ}}{RT} + \frac{\Delta S^{\circ}}{R} \tag{17}$$

where free energy change (ΔG°), enthalpy change (ΔH°), and entropy change (ΔS°) are the thermodynamic constants. T is the absolute temperature (K), R is the gas constant (8.314 J/mol/K) and K_C is the distribution coefficient given by (Eq. (18)):

$$K_C = \frac{q_e}{C_e} \tag{18}$$

The endothermic nature of the biosorption process was also confirmed by the positive enthalpy change (ΔH°). The increased randomness at the solid–solution interface is revealed during the fixation of the Cr(VI) ions on the active sites of the biosorbent based on the positive value of ΔS° [21,22]. The values of enthalpy change (ΔH°) and entropy change (ΔS°) were calculated based on the slope and intercept of the plot of $\log K_C$ vs. $1/T$ (Fig. 21). Free energy change values (ΔG°) are calculated using Eq. (16).

Table 7 highlights the thermodynamic parameters calculated from the batch experiment that shows both positive and negative free energy change values for LC1 biosorbent representing both thermodynamically feasible spontaneous and non-spontaneous nature of the biosorption. But the free energy value for LC2 biosorbent, which was found to be negative, suggests only the spontaneous nature of biosorption with thermodynamic feasibility.

3.10. Regeneration studies

On varying the desorbing solution concentration from 0.02 to 0.2 N, desorption efficiency increases

Table 7
Parameters derived from thermodynamic studies for the biosorption of Cr(VI) on LC1 and LC2 biosorbent

	Thermodynamic parameters at different temperatures for initial Cr(VI) concentration of 400 mg/L			
Type of biosorbent	Temperature (K)	ΔG (kJ/mol)	ΔS (kJ/mol/K)	ΔH (kJ/mol)
LC1	303	1.45	0.131	41.6
	313	0.55		
	323	−1.20		
	333	−2.42		
LC2	303	−4.00	0.074	18.08
	313	−5.96		
	323	−6.15		
	333	−6.34		

from 12 to 60% (figure not shown). Five cycles of biosorption–desorption were experimented with the fixed biosorbent concentration. Experiments conducted on both LC1 and LC2 biosorbents exhibited the same results at 50 mg/L concentration Cr(VI) solution. This proves the possibility of reusing the biosorbent and scaling up to industrial operations. However, further experimentation on desorption is required by investigating the use of different desorbing solutions to achieve 100% desorption. This will ensure the wide applicability and reuse of the biosorbent in the industrial wastewater.

4. Conclusions

In the present research, the acid-treated biomass was prepared to remove the chromium ions from the aqueous solution. The selected biosorbent was proved to be effective in removing hexavalent chromium from aqueous solutions, out of which acid pretreated biosorbent performed better than raw biosorbent. The biosorption capacity of this newly prepared biosorbent (LC2) was found to be high. However, raw biosorbent also yielded a reasonably higher uptake capacity value on comparison with other experimented biosorbents. This shows the potential of using the selected biosorbent in chemical process industries releasing wastewater-containing hexavalent chromium. The biosorbent yields higher efficiency at lower concentrations and could also be recommended for small-scale electroplating units. Langmuir model better described the biosorption equilibrium than other experimental models, which indicates the adsorption of metal ions onto the adsorbent was due to monolayer adsorption. Kinetic studies show that pseudo-second-order kinetic model better obeyed than intraparticle diffusion and pseudo-first-order model, implying chemisorption mechanism. Thermodynamic studies reveal the spontaneous nature of the biosorption in LC2 biosorbent. Nevertheless, LC1 biosorbent pronounces both spontaneous and non-spontaneous biosorption. In addition, endothermic nature of the biosorption and increased randomness at the solid–solution interface was also identified in the study. Batch level studies obtained satisfied results in the optimized experimental conditions and further scaling up the process to industrial wastewater system has to be investigated.

References

[1] B.M. Weckhuysen, I.E. Wachs, R.A. Schoonheydt, Surface chemistry and spectroscopy of chromium in inorganic oxides, Chem. Rev. 96 (1996) 3327–3350.

[2] F.A. Al-Khaldi Ihsanullah, B. Abu-Sharkh, A.M. Abulkibash, M.I. Qureshi, T. Laoui, M.A. Atieh, Effect of acid modification on adsorption of hexavalent chromium Cr(VI) from aqueous solution by activated carbon and carbon nanotubes, Desalin. Water Treat. (in press), doi: 10.1080/19443994.2015.1021847.

[3] D. Mohan, C.U. Pittman Jr., Activated carbons and low cost adsorbents for remediation of tri- and hexavalent chromium from water, J. Hazard. Mater. 137 (2006) 762–811.

[4] M. Chrysochoou, P. Johnston, Reduction of chromium (VI) in saturated zone sediments by calcium polysulfide and nanoscale zerovalent iron derived from green tea extract, GeoCongress 2012 (2012) 3959–3967.

[5] B. Dhal, H.N. Thatoi, N.N. Das, B.D. Pandey, Chemical and microbial remediation of hexavalent chromium from contaminated soil and mining/metallurgical solid waste: A review, J. Hazard. Mater. 250–251 (2013) 272–291.

[6] U.S. Environmental Protection Agency, Toxicological Review of Hexavalent Chromium, National Center for Environmental Assessment, Office of Research and Development, Washington, DC, 1998.

[7] R.J. Irwin, M.V.N. Mouwerik, L. Stevens, M.D. Seese, W. Basham, Environmental Contaminants Encyclopedia Chromium (VI) (Hexavalent Chromium) Entry, National Park Service, Water Resources Division, Fort Collins, CO, 1971.

[8] M.A. Shouman, N.A. Fathy, S.A. Khedr, A.A. Attia, Comparative biosorption studies of hexavalent chromium ion onto raw and modified palm branches, Adv. Phys. Chem. 2013 (2013) 1–9.

[9] D. Mohan, K.P. Singh, V.K. Singh, Trivalent chromium removal from wastewater using low cost activated carbon derived from agricultural waste material and activated carbon fabric cloth, J. Hazard. Mater. 135 (2006) 280–295.

[10] Y. Abatneh, O. Sahu, Removal of chromium by biosorption method (chitosan), Int. Lett. Nat. Sci. 8 (2014) 44–55.

[11] S.K. Das, A.K. Guha, Biosorption of chromium by *Termitomyces clypeatus*, Colloids Surf., B 60 (2007) 46–54.

[12] P.F. Nguema, Z. Luo, J. Lian, The biosorption of Cr (VI) ions by dried biomass obtained from a chromium-resistant bacterium, Front. Chem. Sci. Eng. 8 (2014) 454–464.

[13] L. Velásquez, J. Dussan, Biosorption and bioaccumulation of heavy metals on dead and living biomass of *Bacillus sphaericus*, J. Hazard. Mater. 167 (2009) 713–716.

[14] B. Volesky, Biosorption process simulation tools, Hydrometallurgy 71 (2003) 179–190.

[15] I. Michalak, K. Chojnacka, A. Witek-Krowiak, State of the art for the biosorption process—A review, Appl. Biochem. Biotechnol. 170 (2013) 1389–1416.

[16] D. Park, Y.S. Yun, J.M. Park, Reduction of hexavalent chromium with the brown seaweed *Ecklonia* biomass, Environ. Sci. Technol. 38 (2004) 4860–4864.

[17] A. Zubair, H.N. Bhatti, M.A. Hanif, F. Shafqat, Kinetic and equilibrium modeling for Cr(III) and Cr(VI) removal from aqueous solutions by *Citrus reticulata*

waste biomass, Water Air Soil Pollut. 191 (2008) 305–318.
[18] G. Moussavi, B. Barikbin, Biosorption of chromium (VI) from industrial wastewater onto pistachio hull waste biomass, Chem. Eng. J. 162 (2010) 893–900.
[19] J.A. Fernández-López, J.M. Angosto, M.D. Avilés, Biosorption of hexavalent chromium from aqueous medium with Opuntia Biomass, Sci. World J. 2014 (2014) 8 p.
[20] C. Namasivayam, M.V. Sureshkumar, Removal of chromium(VI) from water and wastewater using surfactant modified coconut coir pith as a biosorbent, Bioresour. Technol. 99 (2008) 2218–2225.
[21] R. Zhang, B. Wang, H. Ma, Studies on chromium(VI) adsorption on sulfonated lignite, Desalination 255 (2010) 61–66.
[22] S. Rangabhashiyam, N. Selvaraju, Evaluation of the biosorption potential of a novel *Caryota urens* inflorescence waste biomass for the removal of hexavalent chromium from aqueous solutions, J. Taiwan Inst. Chem. Eng. 47 (2015) 59–70.
[23] M.Y. Arıca, İ. Tüzün, E. Yalçın, Ö. İnce, G. Bayramoğlu, Utilisation of native, heat and acid-treated microalgae *Chlamydomonas reinhardtii* preparations for biosorption of Cr(VI) ions, Process Biochem. 40 (2005) 2351–2358.
[24] J. Yang, B. Volesky, Modeling uranium-proton ion exchange in biosorption, Environ. Sci. Technol. 33 (1999) 4079–4085.
[25] T. Venkatachalam, V. Kishorkumar, P. Kalaiselvi, A.O. Maske, N. Senthilkumar, Physicochemical and preliminary phytochemical studies on the *Lantana camara* (L.) fruits, Int, J. Pharm. Sci. 3 (2011) 52–54.
[26] R. Elangovan, L. Philip, K. Chandraraj, Biosorption of chromium species by aquatic weeds: Kinetics and mechanism studies, J. Hazard. Mater. 152 (2008) 100–112.
[27] M. Bansal, U. Garg, D. Singh, V.K. Garg, Removal of Cr(VI) from aqueous solutions using pre-consumer processing agricultural waste: A case study of rice husk, J. Hazard. Mater. 162 (2009) 312–320.
[28] M.E. Mahmoud, R.H.A. Mohamed, Biosorption and removal of Cr(VI)–Cr(III) from water by eco-friendly gelatin biosorbent, J. Environ. Chem. Eng. 2 (2014) 715–722.
[29] M. Bhaumik, A. Maity, V.V. Srinivasu, M.S. Onyango, Enhanced removal of Cr(VI) from aqueous solution using polypyrrole/Fe_3O_4 magnetic nanocomposite, J. Hazard. Mater. 190 (2011) 381–390.
[30] N.H. Mthombeni, M.S. Onyango, O. Aoyi, Adsorption of hexavalent chromium onto magnetic natural zeolite-polymer composite, J. Taiwan Inst. Chem. Eng. 50 (2015) 242–251.
[31] V.K. Gupta, A. Rastogi, A. Nayak, Adsorption studies on the removal of hexavalent chromium from aqueous solution using a low cost fertilizer industry waste material, J. Colloid Interface Sci. 342 (2010) 135–141.
[32] T.A. Rearte, P.B. Bozzano, M.L. Andrade, A. Fabrizio de Iorio, Biosorption of Cr(III) and Pb(II) by *Schoenoplectus californicus* and Insights into the binding mechanism, Isrn. Chem. Eng. 2013 (2013) 13.
[33] V.K. Gupta, A. Rastogi, Biosorption of hexavalent chromium by raw and acid-treated green alga *Oedogonium hatei* from aqueous solutions, J. Hazard. Mater. 163 (2009) 396–402.
[34] I. Ullah, R. Nadeem, M. Iqbal, Q. Manzoor, Biosorption of chromium onto native and immobilized sugarcane bagasse waste biomass, Ecol. Eng. 60 (2013) 99–107.
[35] I. Langmuir, The constitution and fundamental properties of solids and liquids. Part I. Solids, J. Am. Chem. Soc. 38 (1916) 2221–2295.
[36] I. Langmuir, The constitution and fundamental properties of solids and liquids. II. Liquids. 1, J. Am. Chem. Soc. 39 (1917) 1848–1906.
[37] I. Langmuir, The adsorption of gases on plane surfaces of glass, mica and platinum, J. Am. Chem. Soc. 40 (1918) 1361–1403.
[38] K. Nithya, A. Sathish, T. Ramachandran, Batch, kinetic and equilibrium studies of chromium(VI) from aqueous phase using activated carbon derived from *Lantana camara* fruit, Orient. J. Chem. 31 (2015) 2319–2326.
[39] K.R. Hall, L.C. Eagleton, A. Acrivos, T. Vermeulen, Pore- and solid-diffusion kinetics in fixed-bed adsorption under constant-pattern conditions, Ind. Eng. Chem. Fundam. 5 (1966) 212–223.
[40] K. Vijayaraghavan, T.V.N. Padmesh, K. Palanivelu, M. Velan, Biosorption of nickel(II) ions onto *Sargassum wightii*: Application of two-parameter and three-parameter isotherm models, J. Hazard. Mater. 133 (2006) 304–308.
[41] Y.G. Bermúdez, I.L.R. Rico, E. Guibal, M.C. de Hoces, M.Á. Martín-Lara, Biosorption of hexavalent chromium from aqueous solution by *Sargassum muticum* brown alga, application of statistical design for process optimization, Chem. Eng. J. 183 (2012) 68–76.
[42] F. Haghseresht, G. Lu, Adsorption characteristics of phenolic compounds onto coal-reject-derived adsorbents, Energy Fuels 12 (1998) 1100–1107.
[43] K.Y. Foo, B.H. Hameed, Insights into the modeling of adsorption isotherm systems, Chem. Eng. J. 156 (2010) 2–10.
[44] S.P. Karthick, K.V. Radha, Equilibrium, isotherm, kinetic and thermodynamic adsorption studies of tetracycline hydrochloride onto commercial grade granular activated carbon, Int. J. Pharm.Sci. 7 (2014) 42–91.
[45] A.O. Dada, A.P. Olalekan, A.M. Olatunya, O. Dada, Langmuir, Freundlich, Temkin and Dubinin–Radushkevich isotherms studies of equilibrium sorption of Zn^{2+} unto phosphoric acid modified rice husk, J. Appl. Chem. 3 (2012) 38–45.
[46] M. Hosseini, S.F.L. Mertens, M. Ghorbani, M.R. Arshadi, Asymmetrical Schiff bases as inhibitors of mild steel corrosion in sulphuric acid media, Mater. Chem. Phys. 78 (2003) 800–808.
[47] Z. Chen, W. Ma, M. Han, Biosorption of nickel and copper onto treated alga (*Undaria pinnatifida*): Application of isotherm and kinetic models, J. Hazard. Mater. 155 (2008) 327–333.
[48] P. Senthil Kumar, K. Kirthika, Equilibrium and kinetic study of adsorption of nickel from aqueous solution onto bael tree leaf powder, J. Eng. Sci. Technol. 4 (2009) 351–363.
[49] A.B. Albadarin, A.H. Al-Muhtaseb, N.A.Al-laqtah, G.M. Walker, S.J.Allen, M.N.M.Ahmad, Biosorption of toxic chromium from aqueous phase by lignin: mechanism, effect of other metal ions and salts, Chem. Eng. J. 169 (2011) 20–30.

[50] A. Dąbrowski, Adsorption—From theory to practice, Adv. Colloid Interface Sci. 93 (2001) 135–224.
[51] S. Lagergren, About the theory of so-called adsorption of soluble substances, Kungliga Svenska Vetensk Handl. 24 (1898) 1–39.
[52] P. SenthilKumar, S. Ramalingam, V. Sathyaselvabala, S. Kirupha, S. Sivanesan, Removal of copper(II) ions from aqueous solution by adsorption using cashew nut shell, Desalination 266 (2011) 63–71.
[53] J. Ye, H. Yin, B. Mai, H. Peng, H. Qin, B. He, N. Zhang, Biosorption of chromium from aqueous solution and electroplating wastewater using mixture of *Candida lipolytica* and dewatered sewage sludge, Bioresour. Technol. 101 (2010) 3893–3902.
[54] D.P. Mungasavalli, T. Viraraghavan, Y.-C. Jin, Biosorption of chromium from aqueous solutions by pretreated *Aspergillus niger*: Batch and column studies, Colloids Surf., A 301 (2007) 214–223.
[55] M.H. Khani, A.R. Keshtkar, M. Ghannadi, H. Pahlavanzadeh, Equilibrium, kinetic and thermodynamic study of the biosorption of uranium onto *Cystoseria indica* algae, J. Hazard. Mater. 150 (2008) 612–618.
[56] X.S. Wang, L.F. Chen, F.Y. Li, K.L. Chen, W.Y. Wan, Y.J. Tang, Removal of Cr(VI) with wheat-residue derived black carbon: Reaction mechanism and adsorption performance, J. Hazard. Mater. 175 (2010) 816–822.
[57] N.A. Fathy, S.T. El-Wakeel, R.R.A. Abd El-Latif, Biosorption and desorption studies on chromium(VI) by novel biosorbents of raw rutin and rutin resin, J. Environ. Chem. Eng. 3 (2015) 1137–1145.
[58] W.J. Weber, J.C. Morris, Advances in water pollution research: removal of biologically-resistant pollutants from waste waters by adsorption, in: Proceedings of International Conference on Water Pollution Symposium, vol. 2, Pergamon Press, Oxford, 1962, pp. 231–266.
[59] C.Y. Chang, W.T.T. Tsai, C.H. Ing, C.H. Chang, Adsorption of polyethylene glycol (PEG) from aqueous solution onto hydrophobic zeolite, J. Colloid Interface Sci. 260 (2003) 273–279.
[60] H.L. Ehrlic, in: C.L. Brierly (Ed.), Microbial Mineral Recovery (Environmental Biotechnology), McGraw-Hill, New York, NY, 1990, pp. 303–324.
[61] M. Tuzen, A. Sarı, Biosorption of selenium from aqueous solution by green algae (*Cladophora hutchinsiae*) biomass: Equilibrium, thermodynamic and kinetic studies, Chem. Eng. J. 158 (2010) 200–206.
[62] S. Tunali, I. Kiran, T. Akar, Chromium(VI) biosorption characteristics of *Neurospora crassa* fungal biomass, Miner. Eng. 18 (2005) 681–689.
[63] S. Rangabhashiyam, N. Selvaraju, Efficacy of unmodified and chemically modified *Swietenia mahagoni* shells for the removal of hexavalent chromium from simulated wastewater, J. Mol. Liq. 209 (2015) 487–497.
[64] S. Chhikara, R. Dhankhar, Biosorption of Cr(VI) ions from electroplating industrial effluent using immobilized *Aspergillus niger* biomass, J. Environ. Biol. 29 (2008) 773–778.
[65] K. Anbalagan, P. Senthil Kumar, R. Karthikeyan, Adsorption of toxic Cr(VI) ions from aqueous solution by sulphuric acid modified *Strychnos potatorum* seeds in batch and column studies, Desalin. Water Treat. (in press), doi: 10.1080/19443994.2015.1049965.